Designed Synthesis of Transition Metal/ Oxide Hierarchical Peapods Array with the Superior Lithium Storage Performance

Huijuan Zhang[1], Yuanjuan Bai[1], Yan Zhang[1], Xiao Li[1], Yangyang Feng[1], Qing Liu[3], Kai Wu[2] & Yu Wang[1]

[1]School of Chemistry and Chemical Engineering, Chongqing University, 174 Shazheng Street, Shapingba District, Chongqing City, P. R. China, 400044, [2]Beijing National Laboratory for Molecular Sciences, College of Chemistry and Molecular Engineering, Peking University, Beijing, 100871, P. R. China, [3]School of Materials Science and Engineering, Chongqing University, 174 Shazheng Street, Shapingba District, Chongqing City, P. R. China, 400044.

Correspondence and requests for materials should be addressed to Y.W. (wangy@cqu. edu.cn; prospectwy@ gmail.com); K.W. (kaiwu@pku.edu.cn) or Q.L. (qingliu@cqu. edu.cn)

In this report, a novel hierarchical peapoded array with Co_3O_4 nanoparticles encapsulated in graphitized carbon fiber is introduced for the first time. The unique peapoded structure is suitable for the excellent anode in LIBs and demonstrates enhanced rate capability, cyclability and prolonged lifespan, e.g. the specific capacity can reach up to 1150 mAh/g. All the enhanced electrochemical performance is reasonably derived from the peapod-like and aligned conformation. Furthermore, due to the specialty of the structure and the versatility of Co_3O_4, the composite will find more applications in specific catalysis, biomedicine, electronics, optoelectronic engineering and gas sensing. The fabrication strategy developed here is also a rational and universal approach towards peapod-like architecture and has significantly widened the specific functional material domain we created before. In our design, more peapod-like aligned samples with various nanoparticles, e.g. oxides, phosphides, even nitrides, encapsulated in graphitized carbon fibers, have been lifted on the research agenda and the results will be presented soon.

A dvanced hierarchical nanomaterials are well-known to play crucial roles in a great number of applications, such as in the fields of sustainable energy, biotechnology, electronics, medicines and industries[1–3]. Nanostructured composite materials, especially with elaborate design and controlled synthesis, would promisingly exhibit a pronounced synergistic effect, which actually originates from the system's individual components, but transcends the simplistic mixture reasonably based on a combined performance[4]. In particular, aiming at developing the next generation sustainable energy techniques, a large variety of hierarchical nanoscale composites have been successfully synthesized and functionalized in harnessing solar energy, water splitting, supercapacitors and Li-ion batteries (LIBs). Among all the aforementioned techniques, LIBs are generally considered as the unique bridging medium to effectively connect the initial stage of clean energies' harvest and conversion with the terminal consumption of human society[5,6]. With the development of the today's automated and electrified society, an impending demand for electrical storage devices has been listed on the research agenda and the next generation electrochemical energy storage devices, which are typically characteristic of high power and energy densities, enhanced cyclability and accelerated rate capability, are now triggering more and more interests all over the world[7–9].

Currently, electrical energy storage systems, normally LIBs, are suffering from some serious problems, mainly inclusive of electrode materials' pulverization, agglomeration and amorphization with galvanostatic cycling continued, which will definitely lead to deterioration of specific capacity, rate capability and cyclability. The major approaches towards alleviation of these frequently encountered issues are to reduce the active materials to nanoscale, design and synthesize carbon-coated composites or mix the electrode materials with more conductive substances, and dope the electrodes with foreign atoms[10,11]. Unfortunately, all the above strategies are still limited with respect to cyclability and addition of excess carbon black or conducting polymer into the systems[12]. So pursuit of excellent LIBs' electrode materials with high power/energy densities and satisfactory cyclabilities, especially without addition of ancillary materials, ever remains a great challenge to date. Direct growth of one-dimensional (1-D) nanostructures with activity of Li storage on conducting substrates is a good choice, as an

optimized balance among electrolyte diffusion, Li ions exchange between electrolyte and active materials, and charge transfer could be captured[13–16]. For example, Qi and coworkers used to erect tin oxide nanowires array on various conductive substrates for the enhanced LIBs anode[13]. Hu, Maier, et al. designed and fabricated a targeted composite array represented with vanadium oxide nanoparticles being evenly distributed in carbon fibers, and realized the improved Li storage efficiency[14]. Lee and coworkers showed us a hybrid core-shell nanocable array with tin oxide nanowires encapsulated inside as the charge transfer pathway and vanadium oxide layers coating outside as the active material to store Li, and the achieved product ultimately demonstrated a strengthened cyclability and wonderful temperature-dependent stability compared to the other vanadium oxide-based electrode materials[15]. Cui et al. employed chemical vapor deposition (CVD) method to generate Si nonowires array and successfully used it as the high-performance anode in LIBs[16]. Meanwhile, inspired by the previous results in the electrical energy storage and encouraged by the practical demands from our modern society, we ever successfully initiated and developed a mesoporous and single-crystal Co_3O_4 nanobelt array on Ti foil with rationally designed and fabricated $Co(CO_3)_{0.5}(OH)0.11H_2O$ nanobelts array as the precursor, and fulfilled an excellent anode in LIBs[17,18]. Moreover, subsequently we designed and created a peapod-like structure with Co_3O_4 nanoparticles encapsulated in well-graphitized carbon fibers using randomly dispersed $Co(CO_3)_{0.5}(OH)0.11H_2O$ nanobelts as sacrificial templates and glucose molecules as the carbon sources, respectively[19]. Because the obtained peapoded composite has several intriguing characters, such as mesoporosity and good graphitization of the carbon fibers, isolation and monodispersion of the encapsulated Co_3O_4 nanoparticles in the carbon fibers and small size of the peapods down to 30 nm in diameter,

a remarkable performance in LIBs anode was entirely verified, e.g. competitive advantages in lifespan, rate capability, specific capacity, stability and no need for addition of any ancillary materials[19]. Since both of direct growth of nanostructured active materials on conducting substrates and designed synthesis of peapod-like composite materials are capable of enhancing the electrochemical energy storage performance in their own way, a realistic and impending question naturally arises: how can we combine the outstanding properties from the two above-mentioned structures and realize more advanced Li storage performance in one integrated system? To clarify this questioned issue, in this report, we will introduce a novel hierarchical peapods array with superior Li storage efficiency based on a rational design and controllable fabrication strategy.

Results

As described in fig. 1, a feasible synthesis route is clearly demonstrated. Similar to our previous report in targeted fabrication of $Co(CO_3)_{0.5}(OH)0.11H_2O$ nanobelts array on Ti foil, $Co(CO_3)_{0.5}(OH)0.11H_2O$ crystal seeds are firstly formed and rooted on the Ti foil surface, and then nanobelts array will accordingly be oriented and grow up. The underlying physical foundation is that: Ti foil is usually covered with a thin layer of TiO_2 because of the oxidation tendency for the fresh Ti when exposed in air, and the isoelectric point with pH value for TiO_2 often falls into a range of 4.5–6.5[20], so in a strong basic solution, in particular, the high-concentration ammonia similar to ours in this research, a large amount of hydroxyl groups will be formed and evenly distributed on the thin TiO_2 layer, which is the first key factor for the growth of nanobelts array. Interestingly, hydroxyl groups are the important constituent for $Co(CO_3)_{0.5}(OH)0.11H_2O$. Theoretically the earlier-formed $Co(CO_3)_{0.5}(OH)0.11H_2O$ crystal seeds will be anchored or immobilized on the Ti foil
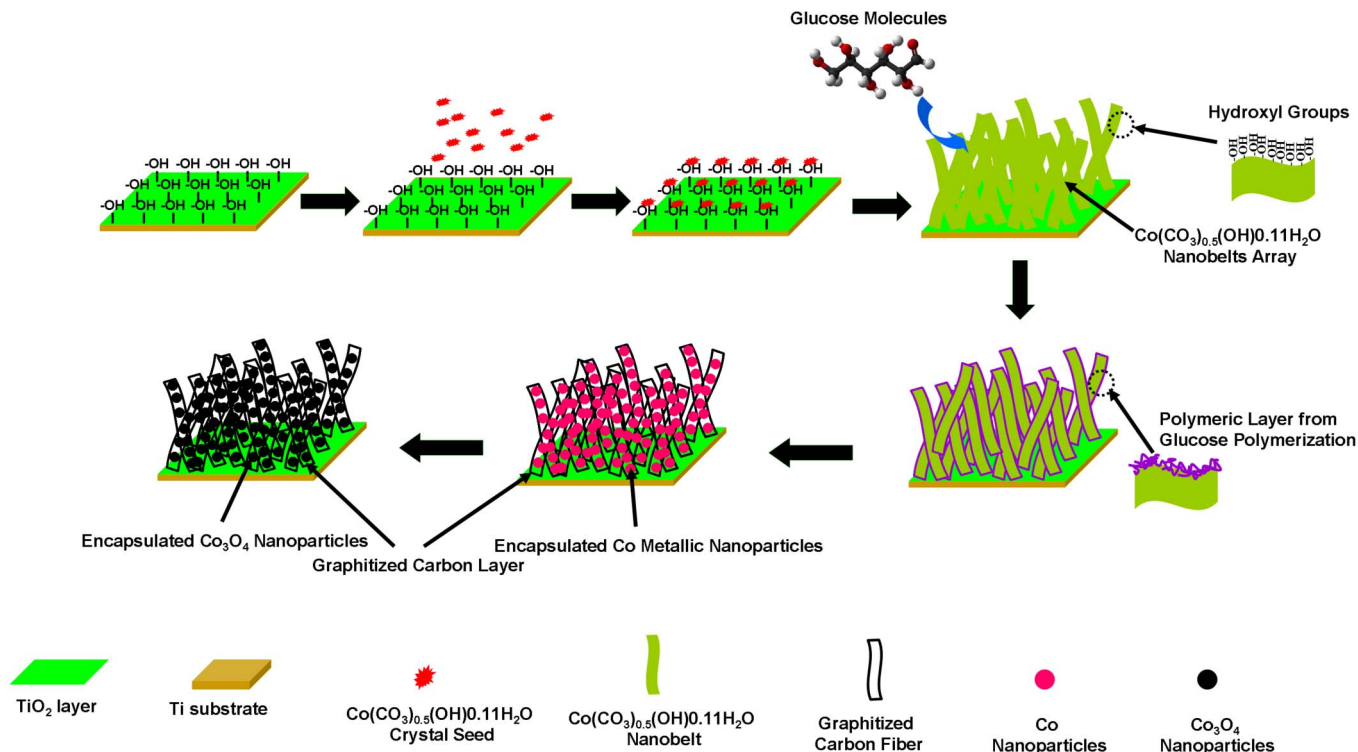

Figure 1 | Schematic illustration for the designed synthesis of hierarchical Co_3O_4 nanoparticles@graphitized carbon peapoded fibers array on Ti foil is presented. In the synthesis, $Co(CO_3)_{0.5}(OH)0.11H_2O$ nanobelts array is firstly designedly erected on Ti foil under hydrothermal condition at 170°C. Then polymeric layers will be uniformly coated on the $Co(CO_3)_{0.5}(OH)0.11H_2O$ nanobelts via the hydrogen bonding action between the glucose molecules and $Co(CO_3)_{0.5}(OH)0.11H_2O$ nanobelts under hydrothermal condition in a proper glucose aqueous solution. Afterwards, experiencing high-temperature calcinations in Ar at 700°C and heat treatment in air at 250°C in sequence, the targeted product of hierarchical Co_3O_4 nanoparticles@graphitized carbon peapoded fibers array on Ti foil is finally achieved (see details in the experimental section).

and then homologous nanobelts array can be fabricated in sequence owing to the growth property of 1-D orientation for $Co(CO_3)_{0.5}$ $(OH)0.11H_2O$. 1-D growth orientation for $Co(CO_3)_{0.5}(OH)0.11$ H_2O is the second key factor to yield the nanobelts array (supporting information)[17]. In the following steps, by referring to the formation of the peapod-like structure, a polymerized layer will be coated across all the $Co(CO_3)_{0.5}(OH)0.11H_2O$ nanobelts surfaces via hydrogen bonding action between glucose molecules and $Co(CO_3)_{0.5}(OH)$ $0.11H_2O$ nanobelts, and the glucose's polymerization process under the hydrothermal condition[19,21–23]. Afterwards, by calcinations of the achieved $Co(CO_3)_{0.5}(OH)0.11H_2O$/polymer nanobelts array in Ar at elevated temperature, peapods array with Co nanoparticles encapsulated in graphitized carbon fibers will be produced. Upon a controlled heat treatment in air, the designed peapods array with active material of Co_3O_4 nanoparticles encapsulated in well-graphitized carbon fibers will be finally obtained.

Identical with the previous results, fabrication of $Co(CO_3)_{0.5}$ $(OH)0.11H_2O$ nanobelts array is highly repeatable and the overall morphology looks like a nanoscale "grassland" covering on Ti foil (supporting information). The nanobelts array exhibits uniformity and continuity, and the individual nanobelt is isolated and separated from each other, which is the prerequisite condition for the following coating polymeric layer (supporting information). If the $Co(CO_3)_{0.5}$ $(OH)0.11H_2O$ nanobelt is peeled off the Ti foil, from fig. 2a of the transmission electron microscopy (TEM) image, we can detect that these nanobelts actually evolve from the same crystal seeds and grow along the same direction. It is gradually that they are diversified with growth going on and develop to some separated nanobelts, however, they are still bound together at the root section to collectively form a large quantity of bundles (fig. 2a). Detailed TEM characterizations further support the claims (supporting information). In fig. 2b, the high-resolution TEM (HRTEM) image, we can find that these $Co(CO_3)_{0.5}(OH)0.11H_2O$ nanobelts are actually single crystal in nature. Two mutually perpendicular interspaces are calculated as 0.302 and 0.441 nm, corresponding to (300) and (001) crystal planes of $Co(CO_3)_{0.5}(OH)0.11H_2O$, respectively. After calcinations of the polymer-coated $Co(CO_3)_{0.5}(OH)0.11H_2O$ nanobelts array in Ar at high temperature, the achieved product of metallic Co nanoparticles@graphitized carbon peapoded fibers array has successfully maintained the original configuration of $Co(CO_3)_{0.5}(OH)0.11H_2O$ nanobelts array (supporting information), implying the potential success in the ultimate yield of Co_3O_4 nanoparticles@graphitized carbon peapoded fibers array. Fig. 3 is a series of the scanning electron microscopy (SEM) images to evidently disclose the morphologies of the Co_3O_4 nanoparticles@graphitized carbon peapoded fibers array. From fig. 3a, the top-view image, a uniform film can be clearly found. In the locally magnified SEM image as shown in fig. 3b, we can

see that many peapod-like 1-D nanostructures are basically aligned together along the same orientation though some of them are partially inter-crossed. In fact, this status matches very well with that of the precursor, $Co(CO_3)_{0.5}(OH)0.11H_2O$ nanobelts array. From fig. 3c, good contact between Co_3O_4 nanoparticles@graphitized carbon peapoded fibers array and Ti foil can be apparently revealed. Only if the Ti foil was toughly bent, the tightly attached peapods array could be partly erected along the edge areas as described in fig. 3d. Upon being peeled off the Ti foil, Co_3O_4 nanoparticles@ graphitized carbon fibers exhibit peapod-like structure as testified in the TEM images of fig. 4a and 4b. In fig. 4a, we can detect that all the products possess peapoded configuration, where isolated nanoparticles are separated from each other and evenly distributed in the carbon fibers with regular interval distance of 5–20 nm. Especially from fig. 4b, such a situation is more clearly solidified in a single peapod. HRTEM image as depicted in fig. 4c, which is collected in the selected boxed area as marked in fig. 4b, reveals a hexagonally patterned crystal structure, which can be attributed to face-centered cubic (fcc) Co_3O_4, and the crystal inter-lattices are calculated to be 0.280 and 0.281 nm, corresponding to $(02\bar{2})$ and $(\bar{2}0\bar{2})$ crystal planes of spinal Co_3O_4, respectively. In addition, from fig. 4c, well graphitized carbon layers can be feathered as well with a thickness of 2–4 nm. Meanwhile, energy-dispersive X-ray spectrum (EDS), Brunauer-Emmett-Teller (BET) and Raman techniques are all applied to determine the co-existence of Co_3O_4 and graphitized carbon (EDS, Raman), and high surface areas up to 241.6 m^2/g and centered pore size distribution at 3.75 nm (BET) (supporting information). In comparison to the characters of Co_3O_4 nanoparticles@ graphitized carbon peapoded fibers, Co nanoparticles@graphitized carbon peapoded fibers demonstrate a distinct crystal structure, where much smaller crystal inter-lattices can be analyzed to derive from fcc metallic Co (supporting information). Nevertheless, it is noteworthy that the thickness of graphitized carbon layers does not vary significantly compared to that of Co_3O_4 nanoparticles@ graphitized carbon peapoded fibers and still remains 2–4 nm, implying the thermal stability of well graphitized carbon and the feasibility of the synthetic strategy in this research. Throughout all the synthesis, X-ray diffraction (XRD) technique is also utilized to trace down the whole transformation process and has successfully recorded the overall transition from $Co(CO_3)_{0.5}(OH)0.11H_2O$ nanobelts array to Co nanoparticles@graphitized carbon peapoded fibers, and finally to Co_3O_4 nanoparticles@graphitized carbon peapoded fibers on Ti foil, further certifying the rationality and reasonability of the designed synthesis of the novel hierarchical Co_3O_4 nanoparticles@graphitized carbon fibers' peapods array on conductive substrate.

In order to attest to the superior performance in Li storage for the designedly synthesized Co_3O_4 nanoparticles@graphitized carbon
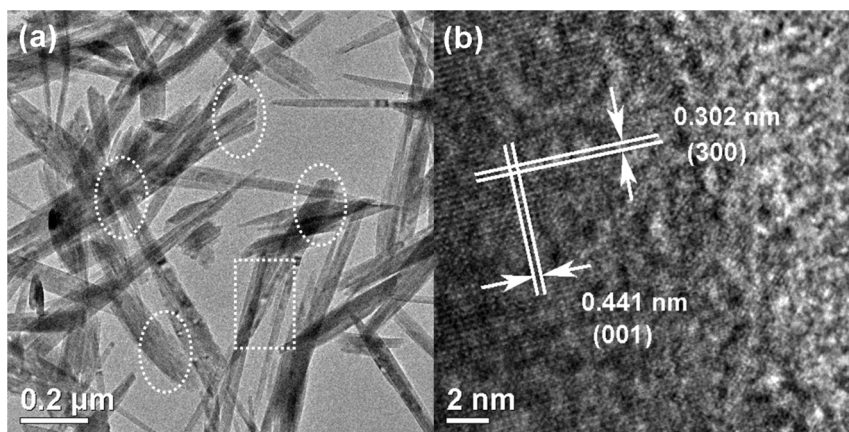

Figure 2 | (a) is the low-magnification TEM image to show the 1-D oriented growth property for the $Co(CO_3)_{0.5}(OH)0.11H_2O$ nanobelts and (b) is the high-resolution TEM (HRTEM) image to clearly show the single-crystal nature for the achieved $Co(CO_3)_{0.5}(OH)0.11H_2O$ nanobelts.
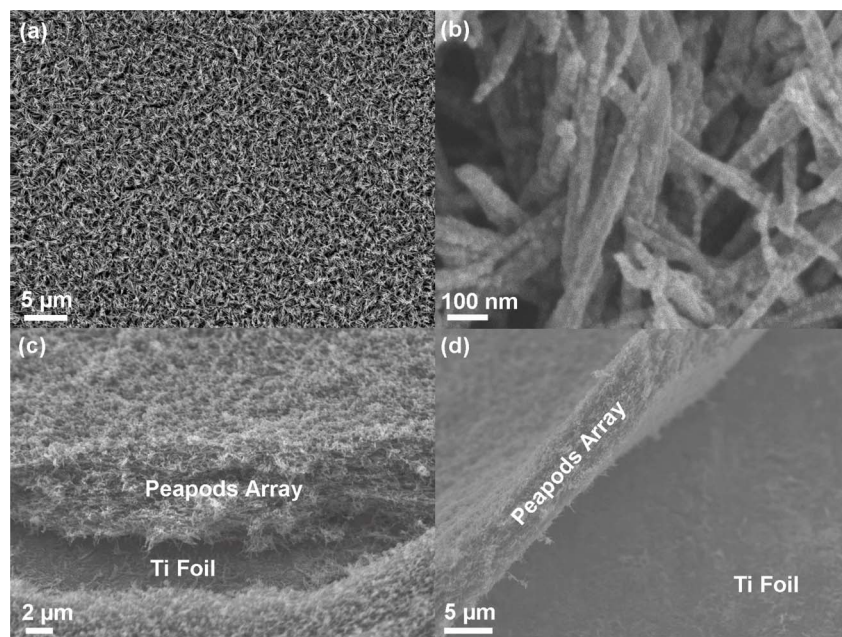
Figure 3 | (a) is the low-magnification SEM image via the top view to reveal the large scale production of the hierarchical Co_3O_4 nanoparticles@ graphitized carbon peapoded fibers array on Ti foil. (b) is the enlarged SEM image to show that the regularly peapoded 1-D structures are aligned together. (c) and (d) are the cross-section views to clearly disclose the uniformity and the attachment to Ti foil for the peapods array.

peapoded fibers array, a series of electrochemical tests have been carried out. As shown in fig. 5a, the cyclic voltammetry (CV) measurement is adopted to investigate the chemical conversion process, wherein scanning potential window is falling into the range of 0.01–3.00 V vs. Li^+/Li and the scan rate is fixed as 0.1 mV/s. In the first cycle, the peaks at potentials of 1.20 and 2.10 V vs. Li^+/Li correspond to the reduction of Co_3O_4 to Co and oxidation of Co to Co_3O_4, respectively[24]. In the following cycles, CV profiles tend to be stable and in particular, 2nd and 10th cycles are chosen to positively exhibit the electrochemical stability of the peapods array. The two profiles match very well with each other and only slight fluctuation in some regions occurs, indicating the Co_3O_4 nanoparticles@graphitized carbon peapoded fibers array has successfully maintained the chemical compositional, structural and architectural stability on experiencing a long time scanning. Note that starting from the second cycle, the profiles of the reductive scans are evolved into two peaks around 1.00 and 1.25 V vs. Li^+/Li, implying the changes of the crystallization and amorphization in the encapsulated Co_3O_4 nanoparticles may result in a fine clarification for the electrochemical process so that the gradual chemical conversions from Co_3O_4 to CoO and then from

CoO to Co can be clearly distinguished, which has often been mentioned in the previous reports[25]. Fig. 5b is the description of galvanostatic measurement with working potential vs. specific capacity. In fig. 5b, we can see that, except for the first discharge-charge curve, the others have a strong tendency to be steady, which also matches very well with the CV profiles. Aiming at confirming the enhanced rate capability and cyclability, both long time cycling and high current densities have been imposed on the Co_3O_4 nanoparticles@graphitized carbon peapoded fibers array as depicted in fig. 5c. From Fig. 5c we can find that a very stable capacity of 1150 mAh/g is delivered over 200 cycles at a charge-discharge rate of 100 mA/g, except for the first one up to 1800 mAh/g. The irreversible capacity is rationally believed to originate from the inevitable formation of solid-electrolyte-interface (SEI) owing to the decomposition of electrolyte, especially for transition metal oxides, e.g. Co_3O_4, when cycled as the anode candidate in LIBs[26]. Subsequently, with the current densities gradually increased to 0.5, 1, 2, and 10 A/g for 20 cycles, respectively, the corresponding deliverable capacities also vary from 800, 760, 730 to 450 mAh/g accordingly, evidently affirming the wonderful rate capability. Finally when the current density is cycled back to
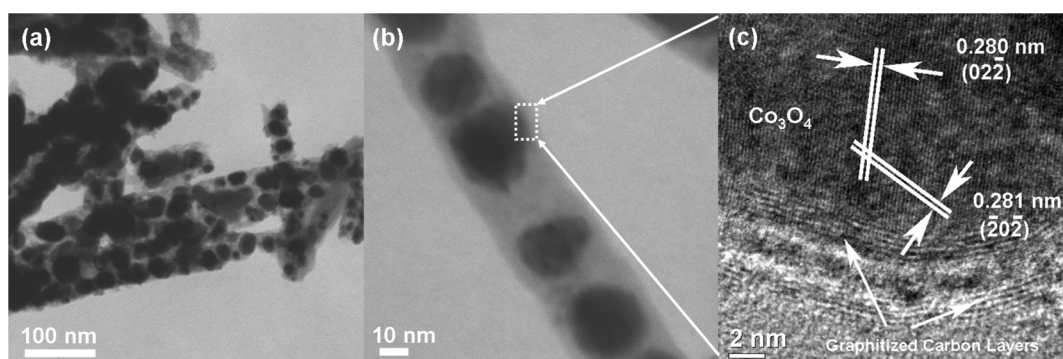

Figure 4 | (a) is the low-magnification TEM image to show the achieved Co_3O_4 nanoparticles@graphitized carbon peapods array after being removed from Ti foil. (b) is the locally magnified TEM image to further confirm the peapoded structure and (c) is the HRTEM image to characterize the crystal structures of the encapsulated Co_3O_4 nanoparticles and the graphitized carbon fibers from the selected area in (b).
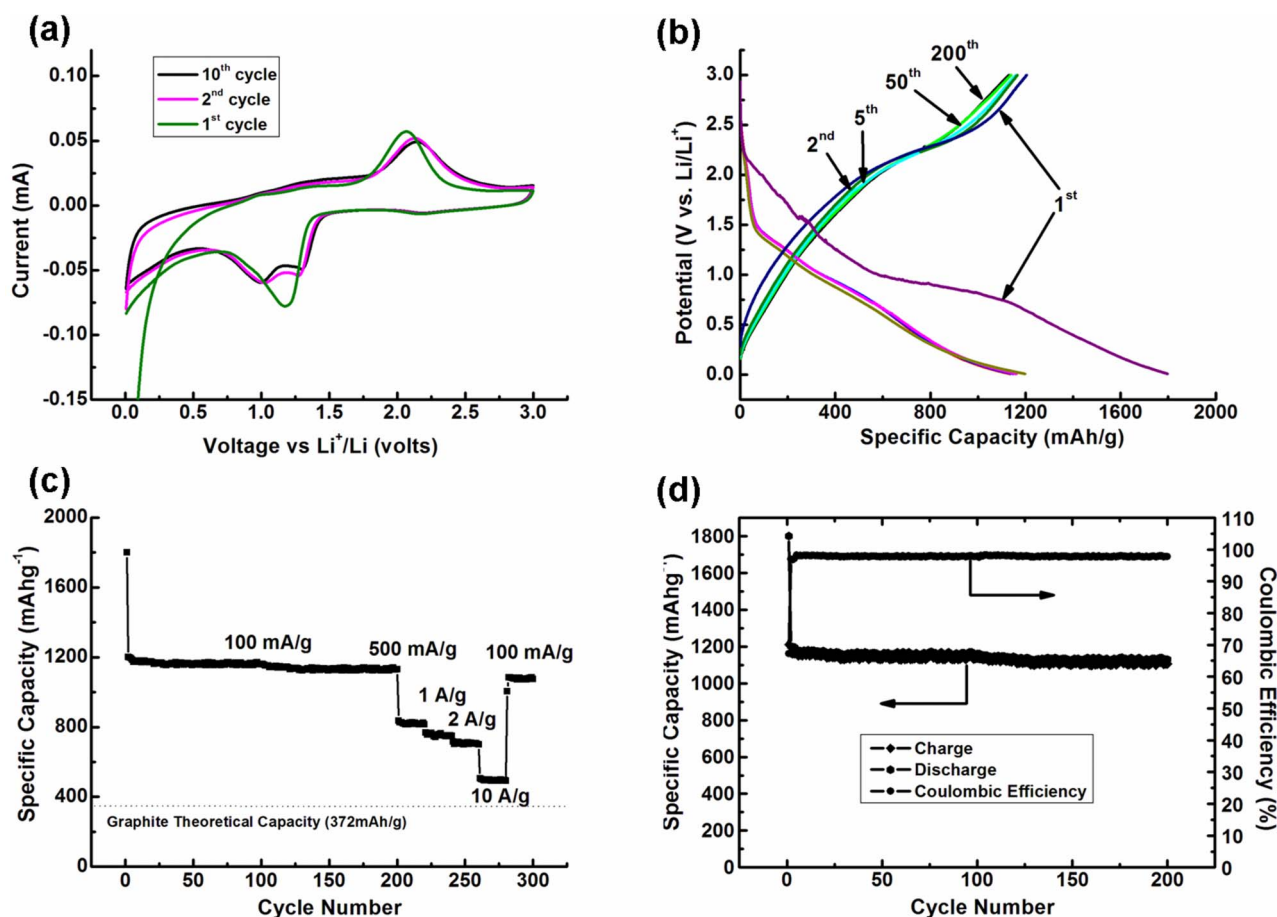
Figure 5 | (a) is the cyclic voltammetry (CV) profile for the hierarchical Co$_3$O$_4$ nanoparticles@graphitized carbon peapoded fibers array on Ti foil, verifying the thermodynamic stability in electrochemical cycling. (b) is the galvanostatic measurement curve at a current density of 100 mA/g. (c) is the long time and rate capability test on the hierarchical Co$_3$O$_4$ nanoparticles@graphitized carbon peapoded fibers array on Ti foil and (d) is the corresponding coulombic efficiency.

100 mA/g, the recoverable capacity can still reach up to 1090 mAh/g and the capacity retention is as high as 95%, indicating the enhanced cyclability, stability and recoverability for the Co$_3$O$_4$ nanoparticles@ graphitized carbon peapoded fibers array when cycled at very high current densities and for a long time running. To the best of our knowledge, it is the most strengthened Li storage performance for Co$_3$O$_4$-based materials for LIBs anode and also outstanding even compared to the other freshly-emerging advanced anodic materials in LIBs[27]. In fig. 5d, a coulombic efficiency very close to 100% is revealed when run at a rate of 100 mA/g other than the first cycle, to further support the claim that the designedly synthesized Co$_3$O$_4$ nanoparticles@graphitized carbon peapoded fibers array is a promising superior anode candidate for the next generation LIBs. Furthermore, temperature-dependent Li storage performance has been investigated as well, where the delivered capacity after 200 cycles run at 100 mA/g is gradually increased with the testing temperature varying from 0, to 25 and 50°C (supporting information).Meanwhile, the Co$_3$O$_4$ nanoparticles@graphitized carbon peapoded fibers array is still characteristic of the superior cyclability and stability, which is the solid guarantee to meet the requirement of the advanced LIBs[15]. The overall Li storage performance for the Co$_3$O$_4$ nanoparticles@graphitized carbon peapoded fibers array is much better than the mesoporous, single crystal Co$_3$O$_4$ nanobelts array or the randomly dispersed Co$_3$O$_4$ nanoparticles@graphitized carbon fibers' peapods, implying a synergistic effect plays a crucial role in Li storage[21].

Discussion

In this research, the targeted hierarchical Co$_3$O$_4$ nanoparticles@graphitized carbon peapoded fibers array on Ti foil possesses unique structure and architecture as revealed in fig. 6. In Li storage, the electrolyte can fluently percolate inwards/outwards the peapods array via the interval space among the aligned peapods and thereby completely soak the active materials[13–17]. The outer well-graphitized carbon fibers of the peapods are directly erected on the conductive substrate of Ti foil so that they can efficiently conduct the charge through the shortcut between the active materials and current collector[19,28]; meanwhile, the carbon fibers can protect the encapsulated Co$_3$O$_4$ nanoparticles from agglomeration and aggregation during galvanostatic cycling, which is significantly favorable for the capacity retention of Li storage, especially under high current densities and is objectively meaningful for the improvement of rate capability[21,29]. In addition, the mesoporous structure, high surface areas and small size of the peapods with 30 nm in diameter will greatly accelerate the electrolyte's penetration and Li ions' exchange rate and will considerably facilitate the rate-limiting step for most of electrochemical systems, e.g. Li ion batteries, fuel cells and supercapacitors, which is also the driving force and deep reason to achieve the superior Li storage performance for the Co$_3$O$_4$ nanoparticles@graphitized carbon peapoded fibers array[15,19,21,30]. The Co$_3$O$_4$ nanoparticles@graphitized carbon peapoded fibers array inherits all the attractive characters in both mesoporous, single crystal Co$_3$O$_4$ nanobelts array and randomly dispersed Co$_3$O$_4$ nanoparticles@graphitized carbon
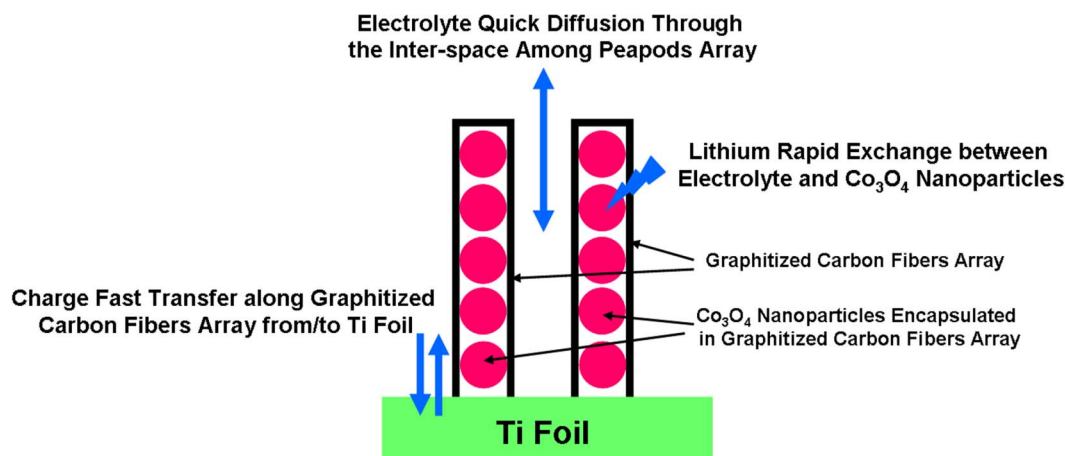
Figure 6 | The mechanism illustrative image is presented to systematically reveal the exact reason of the superior Li storage performance for the hierarchical Co_3O_4 nanoparticles@graphitized carbon peapoded fibers array on Ti foil, where an optimized balance among electrolyte diffusion, charge transfer and Lithium ions exchange has been sought after.

fibers peapods[17,19]. In comparison, the randomly dispersed Co_3O_4 nanoparticles@graphitized carbon fibers peapods only can deliver a specific capacity of 1050 mAh/g within 50 cycles and would decay to 800 mAh/g after tens of cycles at increased current densities[19]. The mesoporous, single crystal Co_3O_4 nanobelts array demonstrated even poorer at the same cycling conditions[17]. The final results reveal that the Co_3O_4 nanoparticles@graphitized carbon peapoded fibers array exhibits a synergistic effect and outperform both of them in Li storage. In the characterizations of Li storage, around 1 cm^2 samples are employed and much more samples can be fabricated dependent on the dimension of Ti foil and the size of the reactor (supporting information), indicating the possibility of large scale production of the Co_3O_4 nanoparticles@graphitized carbon peapoded fibers array via wet-chemistry, the cost-effective approach.

In summary, a novel and hierarchical Co_3O_4 nanoparticles@graphitized carbon peapoded fibers array on Ti foil has been elaborately designed and successfully synthesized. The unique hierarchical structure combines the intriguing characters from mesoporous, single crystal Co_3O_4 nanobelts array and randomly dispersed Co_3O_4 nanoparticles@graphitized carbon fibers peapods, and demonstrates a superior Li storage performance, including excellent cyclability, rate capability and wonderful temperature-dependent effect. All the enhanced performance is reasonably analyzed to develop from the unique hierarchical structure and architecture, in which every part jointly integrates into a powerful unit and collectively exhibits a synergistic effect in Li storage. Furthermore, some advantages, such as easiness of large production and no need to add the ancillary materials, are also the shining points for the specialized peapods array. This research is providing a well-referred model for the design and fabrication of the next generation LIBs electrodes and is extremely meaningful in chemistry and materials sciences. For the next step, some other similar systems to encapsulate the other active materials' nanoparticles in well-graphitized carbon fibers array on conductive current collectors, will be extensively explored and presented soon.

Methods

Materials and chemicals. All chemicals or materials were used directly without any further purification before use. Ethylene Glycol (Fisher Chemical, 99.99%), Ammonia Hydroxide ($NH_3 \cdot H_2O$, 28–30 wt%, J.T.Baker), Cobalt Nitrate ($Co(NO_3)_2$, 99.9%, Aldrich), Sodium Carbonate (Na_2CO_3, 99.9%, Aldrich), and Titanium Foil (0.127 mm (0.005 inch) thick, annealed, 99%, Alfa Aesar), D(+)-Glucose (Cica-Reagent, Kanto Chemical), metallic Li foil (99.9%, Aldrich).

Synthesis of $Co(CO_3)_{0.5}(OH)0.11H_2O$ nanobelt array on Ti foil. Prior to the synthesis, a Ti foil with size of 1 × 3 cm was rinsed with D.I. water and pure ethanol subsequently or sonically cleaned by a mixture of D.I. water, ethanol and acetone with volume ratio of 1 : 1 : 1 for 10 min. Afterwards, the Ti foil was tilted against the wall of the autoclave at a certain angle, with the interested surface facing down. A little modified solution composed of ethylene glycol, concentrated $NH_3 \cdot H_2O$ (28 wt%), 1 M Na_2CO_3 aqueous solution and 1 M Co $(NO_3)_2$ aqueous solution, was slowly poured into the autoclave. The autoclave was then tightly sealed and left in an oven at 140–170°C for 16–64 hr for reaction. Once the reaction was over, the Ti foil was taken out and dried in a vacuum oven at 40°C for at least 3 hr.

Preparation of Co_3O_4 nanoparticles@graphitized carbon peapoded fibers array on Ti foil. Ti foil with $Co(CO_3)_{0.5}(OH)0.11H_2O$ nanobelts array covered was tightly tilted against the inner wall of a clean 45 ml Teflon liner. Then glucose aqueous solution (5 ml, 1 M) was mixed with additional D.I. water (20 ml) to form a homogeneous solution after 5 min ultrasonication. The above solution was introduced into the above-mentioned 45 ml Teflon-lined autoclave and sealed tightly. Then heated the liner in an electric oven at 180°C for 4 hrs. After that, washed the Ti foil using D. I. water and ethanol, and dried the foil in air at 60°C overnight to remove the residue water and ethanol. Afterwards, the dried samples were loaded into the tube furnace and calcined in Ar atmosphere at 700°C for 200 min with a ramp of 1°C/min. Finally the samples were annealed at 250°C for 200 min in air to oxidize the previously formed Co to Co_3O_4.

Characterization of the samples. Scanning electron microscopy (SEM, FEI, 5 kV), Field Emission Scanning Electron Microscope (FESEM, JEOL, JSM-7600F), transmission electron microscopy coupled with EDS analyzer (TEM, Philips, Tecnai, F30, 300 kV), power X-ray diffraction (XRD, Bruker D8 Advance X-ray diffractometer with Cu Kα radiation), Brunauer-Emmett-Teller surface area measurement (BET, Quantachrome Autosorb-6B surface area & Pore size analyzer), RENISHAW Invia Raman Microscope (voltage (AC) 100–240 V, Power 150 W, UK) were employed to characterize the obtained samples.

Electrochemical characterization. Prior to actual testing, Ti foil with samples of 0.6–0.9 mg/cm^2 covered was firstly cut into smaller pieces with size of 1 × 1 cm and weighed in a high-precision analytical balance (Sartorius, max weight 5100 mg, d = 0.001 mg). The obtained pieces of Ti were then used as electrodes with 1 M $LiPF_6$ in ethylene carbonate and diethyl carbonate (EC-DEC, v/v = 1 : 1) as electrolyte. Celgard 2400 was used as the separator film to isolate the two electrodes. Pure Li foil (99.9%, Aldrich) was accepted to server as counter electrode and reference electrode. The swagelok cell was assembled in an argon-filled glove box where moisture and oxygen concentrations were strictly limited below 0.1 ppm. The electrochemical tests were performed on Neware Battery Testing System in the model of 5 V 5 mA and cyclic voltammetry (CV) was collected using Autolab (model of AUT71740). After testing, the tested Co_3O_4 nanobelt array was removed from the Ti foil by knife, and the Ti foil was completely cleaned by ultrasonication subsequently and then weighed in the analytical balance again. Through this way, the exact sample mass used for Li-ion batteries testing was available.

1. Bianchini, C. & Shen, P. K. Palladium-based electrocatalysts for alcohol oxidation in half cells and in direct alcohol fuel cells. *Chem. Rev.* **109**(9), 4183–4206 (2009).
2. Nagaura, T. & Tozawa, K. K. Lithium ion rechargeable battery. *Prog. Batt. Solar Cells* **9**, 209 (1990).
3. Lee, S. W., Yabuuchi, N., Gallant, B. M., Chen, S., Kim, B. S. *et al.* High-power lithium batteries from functionalized carbon-nanotube electrodes. *Nat. Nanotechnol.* **5**, 531–537 (2010).

4. Wu, X. L., Jiang, L. Y., Cao, F. F., Guo, Y. G. & Wan, L. J. LiFePO$_4$ nanoparticles embedded in a nanoporous carbon matrix: superior cathode material for electrochemical energy-storage devices. *Adv. Mater.* **21**(25–26), 2710–2714 (2009).

5. Arico, A. S., Bruce, P., Scrosati, B., Tarascon, J. M. & Van Schalkwijk, W. Nanostructured materials for advanced energy conversion and storage devices. *Nat. Mater.* **4**, 366–377 (2005).

6. Zhang, H. J. & Wong, C. C. Y. Wang, Crystal engineering of nanomaterials to widen the Lithium ion rocking "express way": a case in LiCoO$_2$. *Cryst. Growth Des.* **12**(11), 5629–5634 (2012).

7. Armand, M. & Tarascon, J. M. Building better batteries. *Nature* **451**, 652–657 (2008).

8. Winter, M. & Brodd, R. J. What are batteries, fuel cells, and supercapacitors? *Chem. Rev.* **104**(10), 4245–4269 (2004).

9. Kang, B. & Ceder, G. Battery materials for ultrafast charging and discharging. *Nature* **458**, 190–193 (2009).

10. Simon, P. & Gogotsi, Y. Materials for electrochemical capacitors. *Nat. Mater.* **7**, 845–854 (2008).

11. Zhan, S. Y., Chen, G., Liu, D. L., Li, A., Wang, C. Z. *et al.* Effects of Cr doping on the structural and electrochemical properties of V$_2$O$_5$. *J. Alloys Compds.* **479**(1–2), 652–656 (2009).

12. Wang, Y. G., Wang, Y. R., Hosono, E., Wang, K. X. & Zhou, H. S. The design of a LiFePO$_4$/Carbon nanocomposite with a core-shell structure and its synthesis by an in situ polymerization restriction method. *Angew. Chem. Int. Ed.* **47**(39), 7461–7465 (2008).

13. Chen, S., Wang, M., Ye, J. F., Cai, J. G., Ma, Y. R. *et al.* Kinetics-controlled growth of aligned mesocrystalline SnO$_2$ nanorod arrays for lithium-ion batteries with superior rate performance. *Nano Research* **6**(4), 243–252 (2013).

14. Hu, Y. S., Liu, X., Müller, J. O., Schlögl, R., Maier, J. *et al.* Synthesis and electrode performance of nanostructured V$_2$O$_5$ by using a Carbon tube-in-tube as a nanoreactor and an efficient mixed-conducting network. *Angew. Chem. Int. Ed.* **48**(1), 210–214 (2009).

15. Yan, J., Sumboja, A., Khoo, E. & Lee, P. S. V$_2$O$_5$ loaded on SnO$_2$ nanowires for high-rate Li ion batteries. *Adv. Mater.* **23**(6), 746–750 (2011).

16. Chan, C. K., Peng, H. L., Liu, G., Mcilwrath, K., Zhang, X. F. *et al.* High-performance lithium battery anodes using silicon nanowires. *Nat. Nanotechnol.* **3**, 31–35 (2008).

17. Wang, Y., Xia, H., Lu, L. & Lin, J. Y. Excellent performance in Lithium-ion battery anodes: rational synthesis of Co(CO$_3$)$_{0.5}$(OH)0.11H$_2$O nanobelt array and its conversion into mesoporous and single-crystal Co$_3$O$_4$. *ACS Nano* **4**(3), 1425–1432 (2010).

18. Wang, Y., Zhang, H. J., Lim, W. X., Lin, J. Y. & Wong, C. C. Designed strategy to fabricate a patterned V$_2$O$_5$ nanobelt array as a superior electrode for Li-ion batteries. *J. Mater. Chem.* **21**, 2362–2368 (2011).

19. Wang, Y., Zhang, H. J., Lu, L., Stubbs, L. P., Wong, C. C. *et al.* Designed Functional Systems from Peapod-like Co@Carbon to Co$_3$O$_4$@Carbon Nanocomposites. *ACS Nano* **4**(8), 4753–4761 (2010).

20. Lee, H. S., Hur, T., Kim, S., Kim, J. H. & Lee, H. I. Effects of pH and surface modification of TiO$_2$ with SiO$_x$ on the photocatalytic degradation of a pyrimidine derivative. *Catal. Today* **84**(3–4), 173–180 (2003).

21. Wang, Y., Bai, Y. J., Li, X., Feng, Y. Y. & Zhang, H. J. A general strategy towards encapsulation of nanoparticles in sandwiched graphene sheets and the synergic effect on energy storage. *Chem. Eur. J.* **19**(10), 3340–3347 (2013).

22. Zhang, H. J., Bai, Y. J., Feng, Y. Y., Li, X. & Wang, Y. Encapsulating magnetic nanoparticles in sandwich-like coupled graphene sheets and beyond. *Nanoscale* **5**, 2243–2248 (2013).

23. Wang, Y., Zhang, H. J., Admar, A. S., Luo, J. Z., Wong, C. C. *et al.* Improved cyclability of lithium-ion battery anode using encapsulated V$_2$O$_3$ nanostructures in well-graphitized carbon fiber. *RSC Adv.* **2**, 5748–5753 (2012).

24. Li, W. Y., Xu, L. N. & Chen, J. Co$_3$O$_4$ Nanomaterials in Lithium-ion batteries and gas sensors. *Adv. Funct. Mater.* **15**(5), 851–857 (2005).

25. Nam, K. T., Kim, D. W., Yoo, P. J., Chiang, C. Y., Meethong, N. *et al.* Virus-enabled synthesis and assembly of nanowires for Lithium ion battery electrodes. *Science* **312**(5775), 885–888 (2006).

26. Larcher, D., Sudant, G., Leriche, J. B., Chabre, Y. & Tarascon, J. M. The electrochemical reduction of Co$_3$O$_4$ in a Lithium cell. *J. Electrochem. Soc.* **149**(3), A234–A241 (2002).

27. Kim, M. G. & Cho, J. Reversible and high-capacity nanostructured electrode materials for Li-ion batteries. *Adv. Funct. Mater.* **19**(10), 1497–1514 (2009).

28. Liu, B. & Aydil, E. S. Growth of oriented single-crystalline rutile TiO$_2$ nanorods on transparent conducting substrates for dye-sensitized solar cells. *J. Am. Chem. Soc.* **131**(11), 3985–3990 (2009).

29. Hu, Y. S., Demir-Cakan, R., Titirici, M. M., Müller, J. O., Schlögl, R. *et al.* Superior storage performance of a Si@SiO$_x$/C nanocomposite as anode material for Lithium-ion batteries. *Angew. Chem. Int. Ed.* **47**(9), 1645–1649 (2008).

30. Chan, C. K., Peng, H. L., Twesten, R. D., Jarausch, K., Zhang, X. F. *et al.* Fast, completely reversible Li insertion in Vanadium Pentoxide nanoribbons. *Nano Lett.* **7**(2), 490–495 (2007).

Acknowlegements

Author contributions

Y. W. raised the idea, designed the experiment, supervised the research and drafted the manuscript, H. Z. carried out the synthesis and most of characterizations, Y. B., Y. Z., X. L., Y. F. finished some morphological characterizations, Y. W., K. W. and Q. L. jointly polished the paper and gave some comments.

Additional information

Supplementary information accompanies this paper at http://www.nature.com/scientificreports

Competing financial interests: The authors declare no competing financial interests.

How to cite this article: Zhang, H. *et al.* Designed Synthesis of Transition Metal/Oxide Hierarchical Peapods Array with the Superior Lithium Storage Performance. *Sci. Rep.* **3**, 2717; DOI:10.1038/srep02717 (2013).